Efficient and Robust Host−Guest Antenna Composite for Light Harvesting

André Devaux,*,[†] Gion Calzaferri,*,[‡] Peter Belser,*,[†] Pengpeng Cao,[†] Dominik Brühwiler,[§] and Andreas Kunzmann[∥]

[†]Department of Chemistry, University of Fribourg, Chemin du Musée 9, CH-1700 Fribourg, Switzerland

[‡]Department of Chemistry and Biochemistry, University of Bern, Freiestrasse 3, CH-3012 Bern, Switzerland

[§]Institute of Chemistry and Biological Chemistry, Zürich University of Applied Sciences, CH-8820 Wädenswil, Switzerland

[∥]Optical Additives GmbH, Flurweg 9, CH-3073 Gümligen, Switzerland

Ⓢ *Supporting Information*

ABSTRACT: We report discovery of a new efficient and robust antenna composite for light harvesting. The organic dye hostasol red (HR) is strongly luminescent in aprotic solvents but only weakly luminescent in potassium zeolite L (ZL) at ambient conditions. We observed a dramatic increase of the luminescence quantum yield of HR−ZL composites if some or all exchangeable potassium cations of ZL are substituted by an organic imidazolium cation (IMZ^+) and if the acceptor HR is embedded in the middle part of the channels, so that it is fully protected by the environment of the perylene dye tb-DXP. This led to the discovery of a highly efficient donor,acceptor-ZL antenna material where tb-DXP acts as donor and HR acts as acceptor. The material has a donor-to-acceptor (D/A) absorption ratio of more than 100:1 and a nearly quantitative FRET efficiency. Synthesis of this host−guest material is reported. We describe a successful procedure for achieving full sealing of the ZL channel entrances such that the guests cannot escape. This new material is of great interest for applications in luminescent solar concentrator (LSC) devices because the efficiency killing self-absorption is very low.
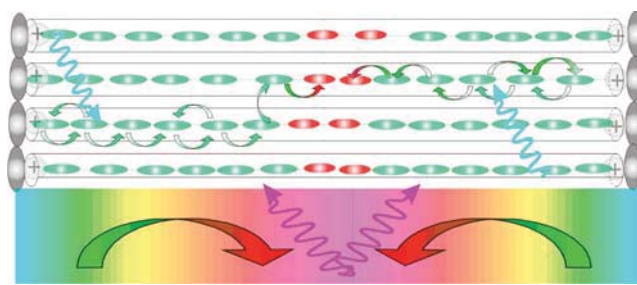
1. INTRODUCTION

Materials that absorb light in the right wavelength range and transfer the electronic excitation energy via radiationless resonance energy transfer to well-positioned acceptors offer unique potential for developing luminescent solar concentrators (LSCs),[1] photoelectronic devices,[2,3] and color-changing media used, for example, in sensing devices and diagnostics.[4,5] They are of great scientific interest for mimicking the antenna system of green plants.[6−9] They have therefore attracted considerable interest by scientists working in different fields. We have succeeded in producing artificial photonic-antenna systems by incorporating dyes into a nanoporous material. The material we chose was zeolite L (ZL), as it has proven to be an ideal host.[4,10,11] The special properties of ZL have also encouraged other researchers in developing highly interesting composite materials.[12−22] ZL crystals are cylindrically shaped porous aluminosilicates featuring hexagonal symmetry.[23,24] The size and aspect ratio of the crystallites can be tuned over a wide range. A nanometer-sized ZL crystal consists of many thousands of one-dimensional channels oriented parallel to the cylinder axis. These can be filled with suitable guest molecules. Geometrical constraints imposed by the host structure led to supramolecular organization of the guests. Thus, very high concentrations of non-interacting or only very

weakly interacting dye molecules can be reached. The channel openings can be plugged with molecules to stop chromophores from leaking out or unwanted molecules from being taken up into the channels. This is a prerequisite for obtaining a material with long-term chemical and photochemical stability. The fully hydrated ZL has the stoichiometry $M_9(SiO_2)_{27}(AlO_2)_9·21H_2O$, where M is a monovalent cation, mostly potassium, needed to compensate for the negative framework charge. Because 3.6 monovalent cations are located in the large channel and can be exchanged either completely or partially by alkali, earth-alkali, and other metal cations, the ionic strength inside of the channels is very high and acidic. While this is desirable for many applications,[25−29] it often causes problems in dye−ZL composites as it has a very strong influence on their spectroscopic, photophysical, and photochemical properties in an ambient temperature regime.[10,12,29−33] Therefore, it was impossible to use acid sensitive dyes, which is a very severe limitation. We tried to overcome this problem for the commercially available dye hostasol red (HR; Table 1), which was expected to have excellent properties as an acceptor in a

Table 1. Structural Formulas of the Organic Compounds Used in This Study

HR   tb-DXP   IMZ[+]
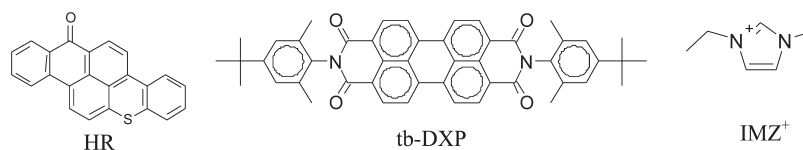
ZL-based antenna material, by using Cs^+ as a co-cation with moderate success.[32] Our findings that the new perylene dye tb-DXP can be very well inserted into the nanochannels of ZL and that the corresponding composites exhibit excellent luminescence properties led to the conclusion that HR would make an ideal acceptor for this dye.[11] This motivated us to reexamine HR–ZL composites and to search for possibilities to tune the nanochannel environment in such a way that HR acts as a strongly luminescent acceptor. We succeeded by exchanging part of the ZL cations by the organic cation 1-ethyl-3-methyl imidazolium (IMZ^+). Furthermore, the acceptor was embedded in the middle part of the channels, as illustrated in Figure 1. In
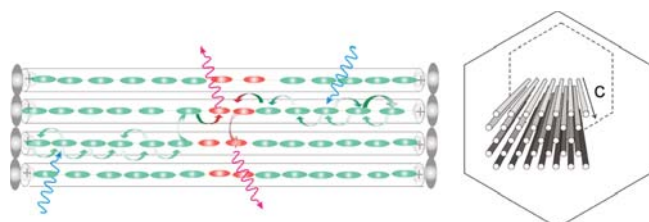

Figure 1. Schematic overview of a ZL-based artificial photonic antenna. (Left) The chromophores are embedded in the channels of the host material. The green dyes act as donor molecules that absorb the incoming light and transport the electronic excitation energy via radiationless resonance energy transfer to the red acceptors, shown in the middle part of the channels. Comparison of the red acceptor to the green emission ratio enables monitoring of the transport process. The channels are plugged with (gray) stopcock molecules to prevent guests from escaping. (Right) Illustration of a bunch of such strictly parallel channels, as found in ZL. The center-to-center distance and the shortest distance between the channels are 1.84 and 0.58 nm, respectively. A unit cell is 0.75 nm long, the pore opening is 0.71 nm wide, and the largest diameter in the channel is 1.26 nm.

this way, the HR is fully protected and mostly exposed to tb-DXP. These procedures led to the discovery of a new efficient and robust host–guest antenna composite for light harvesting that will be reported here.

2. EXPERIMENTAL SECTION

The ZL type most often used in this study was of barrel shape with a length and diameter of about 500 nm. In some cases, nanosized zeolite L (NZL) with a particle size of about 30 nm was used.

It is convenient to describe the dye loading of a dye–ZL composite by means of the occupation probability p, as given by eq 1.

$$p = \frac{\text{number of occupied sites}}{\text{total number of sites}} \qquad (1)$$

The value of p ranges from 0 for an empty ZL to 1 for a fully loaded one. A site expresses the number n_s of unit cells occupied by a guest. It can, for example, be equal to 1, 2, or 3 but is not necessarily an integer. A number in the composite name, such as dye–ZL.05 or dye–ZL.25, indicates the dye loading (occupation probability) of the ZL host. We use $n_s = 3$ for tb-DXP and HR. The dye concentration $c(p)$ in a guest–host composite can be expressed as a function of p as follows:[4,10]

$$c(p) = 0.752 \frac{p}{n_s} \left(\frac{\text{mol}}{\text{L}} \right) \qquad (2)$$

It is sometimes necessary to clearly indicate the charge compensating co-cations present. For example, we write "dye–ZL.5($3.1M1^+,0.5M2^+$)" to indicate that out of the 3.6 exchangeable cations, 3.1 are of $M1^+$ and 0.5 of $M2^+$ type.

2.1. Materials and Chemicals. Cesium-exchanged nanosized ZL (NZL-40) was obtained from Clariant GmbH, while barrel-shaped ZL was prepared according to a procedure that is described below. Clariant GmbH provided a purified sample of Hostasol Red GG (HR). tb-DXP was synthesized according to a newly developed procedure based on previously published works.[34] A detailed description of this procedure will be published in a separate paper. The other chemicals used in this study were obtained from their respective suppliers and used without further purification: aluminum hydroxide (ABCR, dried gel, >99%); Aerosil OX-50 (Degussa); potassium hydroxide (Fluka, purum p.a. >85%); potassium nitrate (Fluka, puriss p.a. ≥99%); 1-ethyl-3-methylimidazolium bromide (IMZ^+, Fluka, ≥97%); 1-butanol (Sigma-Aldrich, puriss p.a.); acetonitrile (Honeywell, gradient grade for HPLC); dichloromethane (DCM; Fluka, puriss, p.a.); toluene (Thommen-Furler AG, technical grade); branched poly ethylenimine (Sigma-Aldrich, M_w = 600–800); ethanol (Honeywell, p.a.); immersion oil (Sigma, for microscopy); base-coat nail varnish (Lady Manhattan Cosmetics, Pro Shine Base Coat). An aqueous solution of hydrofluoric acid (Sigma-Aldrich, technical 40–45%) was diluted to ca. 4% with doubly distilled water before use.

2.2. Synthesis Procedures. *2.2.1. Synthesis of Barrel-Shaped ZL.* Barrel-shaped ZL crystals with an average length and diameter of 500 nm were prepared according to the procedure reported in refs 35 and 36. The synthesis gel had an oxide ratio of 2.83 K_2O to 1.00 Al_2O_3 to 9.83 SiO_2 to 165.6 H_2O. The reactant amounts were chosen so that two 40 mL PTFE pressure vessels could be filled to an operating level corresponding to about three-fourths of the total volume. An aluminate solution (solution A) was prepared by first dissolving 8.1 g of potassium hydroxide in 25.4 g of doubly distilled water. Once the KOH was fully dissolved, 3.5 g of aluminum hydroxide was added, and the solution was refluxed for 16 h. The slightly turbid solution was then cooled to room temperature (rt), and water loss was compensated. The silica solution (solution B) was prepared by adding 30.2 g of doubly distilled water to 12.9 g of Aerosil OX-50. The mixture was dispersed with an Ultra Turrax T18 basic (IKA) for 15 min at 16 000 rpm. The dispersion was left standing at rt for 1 h before dispersing it again for 8 min at 16 000 rpm. After this second dispersion step, solution A was quickly poured into solution B under vigorous stirring. The resulting viscous white gel was aged for 3 min at rt under strong stirring before being evenly split on the two pressure vessels. Crystallization took place in a rotating oven at 160 °C for 42 h with a rotation speed of 20 rpm. Once the reaction was finished, the vessels were cooled in an ice bath for 1 h before being opened. The milky white suspension was centrifuged for 15 min at 3100 rpm. The white residue was then washed with boiling doubly distilled water until the pH of the supernatant was 7. The size distribution and morphology of the obtained ZL crystals was checked by taking SEM images. The images revealed a material nearly identical to the one reported in ref.[35]

2.2.2. Preparation of HR–ZL and HR–ZL(yM$^+$,xIMZ$^+$), M^+ = K^+ or Cs^+. Prior to the gas phase loading procedure, the barrel-shaped ZL was submitted to an ion exchange with either KNO_3 or IMZ^+. In such a procedure, 100 mg of the ZL was suspended in 10 mL of an aqueous solution of KNO_3 or IMZ^+ (c = 0.01 M in both cases). The suspension was left stirring at 70 °C for 18 h. The ZL material was then

centrifuged off (15 min at 2100 rpm) and washed once with 10 mL of deionized water. The nanosized ZL was Cs^+ exchanged in a similar fashion. The gas phase loading procedure for HR was carried out as follows: 100 mg of ion-exchanged ZL (either with K^+, Cs^+, or IMZ^+) and 2.2 mg of HR (corresponding to a target loading of $p = 0.5$) were weighed into a 25 mL round-bottom flask. After the addition of 10 mL of dichloromethane, the mixture was sonicated for 5 s to dissolve the dye and disperse the ZL. The solvent was removed on a rotary evaporator at 40 °C and a pressure of 600 mbar. The HR-coated ZL material was then transferred from the flask into an agate mortar and ground into a fine powder. The powdered material was filled into a glass ampule (25 × 20 mm) and dried on a vacuum line at rt for 24 h at a pressure of 2×10^{-2} mbar. After the ampule was sealed under vacuum, the gas phase insertion process took place in a rotating oven or a salt bath at 270 °C (K^+, Cs^+) or 150 °C (IMZ^+) for 3 d. The ampule was then removed from the heating source and cooled to rt. After opening the ampule, the dye-loaded ZL was washed three times with 20 mL portions of dichloromethane. The supernatant of the third washing showed no traces of HR. The HR−ZL(3.6IMZ$^+$) composite kept its pinkish-red coloring and strong luminescence after longer exposure to humidity, while the Cs^+ and K^+ type quickly changed to a very weakly luminescent violet color (Figure 3B,C). Furthermore, a sample of the HR−ZL(3.6IMZ$^+$) was stored in water for 2 weeks and did not show any color changes or reduction in luminescence intensity (Figure 3D). Effective p of HR was determined by HF analysis (see below).

2.2.3. Preparation of tb-DXP,HR−ZL(yK$^+$,xIMZ$^+$). This composite was synthesized by first loading barrel-shaped ZL with IMZ^+. For this, 100 mg of the ZL was suspended in a mixture of 7.2 mL of deionized water and 2.8 mL of an aqueous stock solution of IMZ^+ ($c = 0.1$ M), and letting it stir for 18 h at 70 °C. The amount of IMZ^+ used here corresponds to a target loading of 4 IMZ^+ per ZL unit cell. The ZL(3.6IMZ$^+$) was collected by centrifugation (15 min at 2100 rpm) and washed once with 10 mL of deionized water. HR was loaded into the ZL(3.6IMZ$^+$) by means of gas phase adsorption with a target loading level of $p = 0.01$. For this, 50 mg of the ZL were mixed with 1.5 mL of an HR stock solution in dichloromethane ($c = 6 \times 10^{-5}$ M) and 8.5 mL of dichloromethane in a 25 mL round-bottom flask. The mixture was dispersed in an ultrasonic bath for 5 s. After the removal of the solvent on a rotary evaporator (40 °C, 600 mbar), the residue was ground to a fine powder in an agate mortar. The powder was dried on a vacuum line at rt at a pressure of 2×10^{-2} mbar for 24 h after being filled into a small glass ampule. Once the ampule was sealed, the insertion took place at 150 °C for 3 d. The HR−ZL(3.6IMZ$^+$) composite was then removed from the ampule and washed once with 10 mL of dichloromethane. Insertion of the donor dye tb-DXP was performed in a similar way: 50 mg of the HR−ZL(IMZ$^+$) was mixed with 1 mg of tb-DXP (corresponding to a target loading of $p = 0.3$) in a 25 mL round-bottom flask. After the addition of 10 mL of dichloromethane, the mixture was dispersed for 5 s in an ultrasonic bath. The solvent was then evaporated on a rotary evaporator (40 °C, 600 mbar). The residue was removed from the flask and ground to a fine powder in an agate mortar. The powder, after being transferred into a small glass ampule, was dried for 24 h at rt on a vacuum line. The sealed ampule was put into a salt bath at 190 °C for 3 days in order to load the tb-DXP. Once the process was complete, the tb-DXP,HR(3.6IMZ$^+$) composite was removed from the ampule and washed three times with 10 mL portions of dichloromethane. The effective p of the two dyes were determined by HF analysis.

2.2.4. Dye−ZL Composite Sealing Procedure. Coating the dye−ZL composites with branched poly ethylenimine (PEI) enabled sealing their entrances. In a typical experiment, 20 mg of the dye−ZL was suspended in 10 mL of toluene by ultrasonic treatment for 10 min. In the case of the HR−ZL(3.6IMZ$^+$) samples, no leaking of HR into the toluene phase was observed. A saturated PEI stock solution in toluene (0.165 mg/mL) was prepared, and 2 mL of this solution was added dropwise to dye−ZL dispersion under sonication. The mixture was submitted to further ultrasonic treatment for 30 min. The coated material was collected through centrifugation (3000 rpm, 15 min) and dried in a vacuum oven (400 mbar) at 85 °C for 18 h.

2.3. Analysis Methods. Absorption spectra were recorded with a Lambda 25 spectrophotometer (PerkinElmer) with a slit width of 1 nm and a scan speed of 120 nm/min. Luminescence spectra were obtained from an LS50B (PerkinElmer) by using a slit width of 7.5 nm for oil−glass sandwiches (OGS) and of 2.5 nm for liquid samples. The scan speed was 120 nm/min. Both spectrometers were equipped with a custom-built sample holder for the OGS samples, as described in ref 11.

2.3.1. Leaking Tests of Sealed Dye−ZL Composites. To monitor the effectiveness of the sealing procedure, we dispersed 15 mg of the ZL composites (both sealed and unsealed) in 5 mL of a 1:1 mixture of acetonitrile and 1-butanol. To ensure a good dispersion, the composite was submitted to an ultrasonic treatment for 5 min. The dispersion was then left stirring at rt for 3 h. Afterward, the composite was centrifuged off, and the supernatant was filtered over a 0.22 μm PTFE syringe filter (Membrane Solutions, MS PTFE Syringe Filter 0.22) to remove any residual small ZL particles. The amount of leaked dye was then determined by measuring the UV−vis spectrum of the filtered supernatant. The PEI sealed dye−ZL composites usually showed no traces of dyes present in the supernatants, while dye leaking is quite significant in the unsealed case.
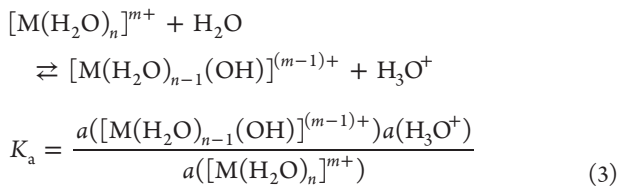
2.3.2. Determination of Loading Levels by HF Analysis. Dissolving the ZL host and measuring the UV−vis absorption of the dyes in the resulting solution allowed determining the effective loading levels of dye−ZL composites. In a first step, 2 mg of the loaded material was dispersed in 3 mL of ethanol (Honeywell, p.a.) in a PS cuvette. Then, 300 μL of a 4% aqueous HF solution was added to the suspension. The ZL host was fully dissolved after 30 min, leaving a clear solution. The loading degree was then calculated from the dye concentrations obtained from the UV−vis absorption spectrum.

2.3.3. Preparation of Oil−Glass Sandwiches (OGS) for Spectroscopy. All absorption and luminescence spectra of dye-loaded ZL composites were recorded from OGS prepared as reported in refs 37 and 38. The samples were prepared by suspending 1 mg of dye-loaded material in 1 mL of 1-butanol. A 200 μL droplet was then deposited on a glass microscopy coverslip (Marienfeld, 24 × 32 mm, No. 1). A steel ring with an inner diameter of 8 mm and an outer diameter of 20 mm and equipped with an O-ring was used to confine the droplet's spread. Once the solvent was fully evaporated, the steel ring was removed, and 300 μL of immersion oil was deposited on the thin ZL layer. Placing a second coverslip on top of the immersion oil and sealing the sides with base-coat nail varnish completed the sandwich.

2.3.4. Relative Quantum Yield Measurements Using OGS. To measure absorption or luminescence spectra, we used a custom-built sample holder designed to ensure that the incident light beam hits the OGS at the same angle of 45° in both the absorption and luminescence spectrometer. This ensures a similar geometry in both measurement types, which is crucial for relative quantum yield determinations. The OGS is placed between two black anodized aluminum plates with the dye−ZL spot centered in the 6 mm hole. The whole assembly is then inserted into the sample holder slit and fixed by tightening two Teflon screws. The anodized black aluminum plates serve as beam limiters and help in avoiding reflection effects from the glass plates. For details of these measurements, we refer to ref 11.
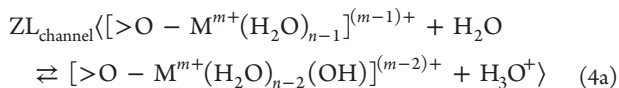
3. RESULTS AND DISCUSSION

The properties of guest-zeolite composites are markedly influenced by the co-cations and the presence or absence of a cosolvent such as water, methanol, toluene or others.[4,32,39,40] In order to describe reactions that take place inside the nano sized channels of ZL we use angle brackets. The expressions have the following form: ZL$_{channel}$ $\langle A + B \rightarrow C \rangle$. We apply this nomenclature to the important observation that all metal cations give acidic solutions in water, according to eq 3, where the symbol a expresses the activity of the involved species:
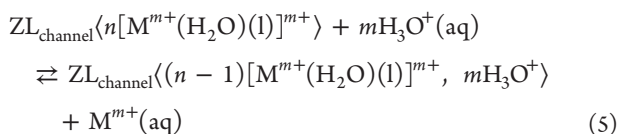
$$[M(H_2O)_n]^{m+} + H_2O$$
$$\rightleftharpoons [M(H_2O)_{n-1}(OH)]^{(m-1)+} + H_3O^+$$

$$K_a = \frac{a([M(H_2O)_{n-1}(OH)]^{(m-1)+})a(H_3O^+)}{a([M(H_2O)_n]^{m+})} \qquad (3)$$

The pK_a values of some selected cations are $Li^+ = 13.6$, $Na^+ = 13.9$, $K^+ = 14.0$, $Be^{2+} = 5.4$, $Mg^{2+} = 11.2$, $Ca^{2+} = 12.7$, and $Eu^{3+} = 8.6$.[41] The acid−base reaction that takes place inside the channels of ZL can be written as eq 4. This equation takes the same form as eq 3 and defines the pK_a in the channels of ZL:

$$ZL_{channel}\langle[M^{m+}(H_2O)_n]^{m+} + H_2O$$
$$\rightleftharpoons [M^{m+}(H_2O)_{n-1}(OH)]^{(m-1)+} + H_3O^+\rangle \qquad (4)$$
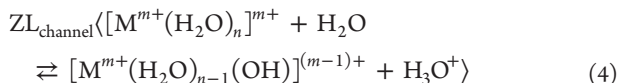
An alternative way to write this equilibrium is to explicitly consider that at least some of the charge compensating cations will bind to an $-Al^{3+}-O^{2-}-Si^{4+}-$ oxygen:

$$ZL_{channel}\langle[>O - M^{m+}(H_2O)_{n-1}]^{(m-1)+} + H_2O$$
$$\rightleftharpoons [>O - M^{m+}(H_2O)_{n-2}(OH)]^{(m-2)+} + H_3O^+\rangle \qquad (4a)$$

As a consequence of this, ZL channels containing metal cations can be free of protons only when completely dry. As soon as water is added, reactions 4 and 4a take place, and the environment becomes more or less acidic, depending on the nature of the metal cation.[32,42] A detailed discussion of this effect is given in the Supporting Information. Inserting pH-sensitive dyes and measuring their UV−vis absorption or fluorescence spectra can be used to determine the Brönsted acidity in the channels. Values measured for some cations are Li^+ (pH = 3.45), K^+ (pH = 3.38), Cs^+ (pH = 3.68), Mg^{2+} (pH = 2.82), and Ca^{2+} (pH = 3.10).[10,32,33] It is useful to remember that the pure water used to wash a ZL sample or a dye−ZL composite should be considered as a 10^{-7} to 10^{-6} M H_3O^+ solution. Such a procedure therefore favors insertion of often unwanted protons, according to eq 5. From the stoichiometry of a fully hydrated ZL, we see that exchange of, for example, one monovalent cation by a proton increases the acidity of the unit cell drastically because the H_3O^+/H_2O ratio becomes 1:21, which is close to the value of 2.5 M hydrochloric acid.[30]

$$ZL_{channel}\langle n[M^{m+}(H_2O)(1)]^{m+}\rangle + mH_3O^+(aq)$$
$$\rightleftharpoons ZL_{channel}\langle(n - 1)[M^{m+}(H_2O)(1)]^{m+},\ mH_3O^+\rangle$$
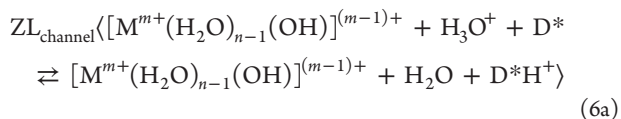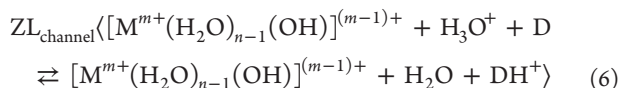$$+ M^{m+}(aq) \qquad (5)$$

An illustrative case that has been studied in some detail is the behavior of HR embedded in ZL. The remarkable color changes of HR−ZL we have observed are illustrated in Figure 2A.

It shows the influence of three different co-cations in the dried samples. Apart from the color change, we found that luminescence is completely quenched in the case of Mg^{2+}, while it is of moderate intensity for K^+ and very intense for Cs^+. K^+ is the co-cation in the samples shown in Figure 2B:[32] the color of the hydrated sample changes upon drying by evacuation (left), and interestingly, the color of the nonluminescent hydrated sample changes after exposure to ammonia vapors (right). It is similar to the color of the dried sample and shows luminescence. The ammonia-induced change is, however, not stable and vanishes after some time due to evaporation of the ammonia. We cannot exclude that the Mg^{2+} might also directly
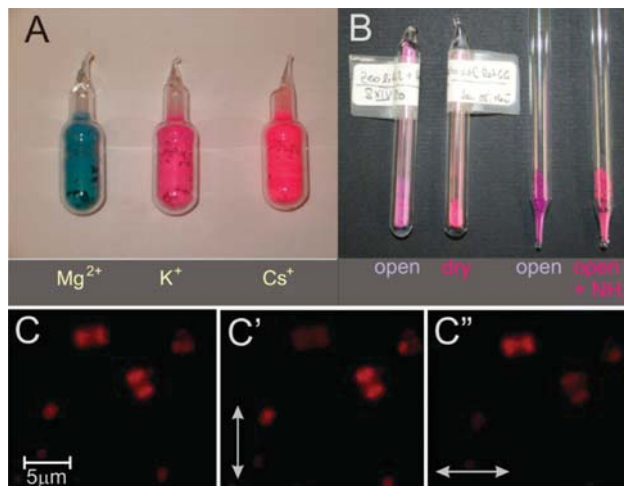
Figure 2. HR−ZL composites. (A) Influence of the co-cation on the color of the dried (evacuated) samples. (B) Samples with K^+ as co-cation. (Left) The color of the hydrated (open) sample changes upon drying by evacuation (dry). (Right) The color of the hydrated sample changes after exposure to ammonia and adopts the same color as seen in the evacuated sample. (C) Fluorescence microscopy images of ZL crystals loaded with HR; (C' and C") observation through a polarizer, the orientation of which is indicated by double arrows.
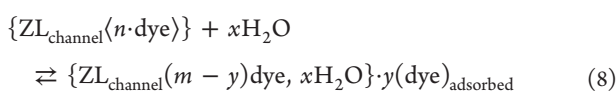
interact with HR. The main reason for the color change and luminescence quenching, however, seems to be the proton activity and not the amount of water present, because otherwise, the influence of the ammonia could not be understood. This can be written as eqs 6 and 6a, in which the symbol D is used for the dye, for example, HR, and D* for the dye in an electronically excited state. The acidity constant pK_a* of a dye in the electronically excited state usually differs from the pK_a in the ground state. For example, the values for the oxazine dye oxonine (Ox^+) are $pK_{a1} = 11.27$, $pK_{a2} = -1.2$, and $pK_{a2}* = 1.2$.[32]

$$ZL_{channel}\langle[M^{m+}(H_2O)_{n-1}(OH)]^{(m-1)+} + H_3O^+ + D$$
$$\rightleftharpoons [M^{m+}(H_2O)_{n-1}(OH)]^{(m-1)+} + H_2O + DH^+\rangle \qquad (6)$$

$$ZL_{channel}\langle[M^{m+}(H_2O)_{n-1}(OH)]^{(m-1)+} + H_3O^+ + D*$$
$$\rightleftharpoons [M^{m+}(H_2O)_{n-1}(OH)]^{(m-1)+} + H_2O + D*H^+\rangle$$
$$(6a)$$

We show in Figure 2C,C',C" fluorescence microscopy images of two crystals that are about 3 μm long. The images observed through a polarizer indicate that the orientation of the dyes electronic transition dipole moment is essentially parallel to the crystal c axis, similar to what has been observed for perylene dyes.[43,44] A general procedure used for inserting neutral dyes into the ZL channels consists of the following steps. The partially dried ZL crystals are suspended in a solution containing the desired amount of dissolved dye. Gentle heating and evacuation evaporate the solvent so that the dye adsorbs homogeneously at the outer surface of the crystals. In a next step, the sample is evacuated under such conditions that solvent and water are removed but no dye is lost. The reaction vessel is then closed and heated to a temperature at which the dye becomes sufficiently mobile to enter the channels. The last step can be expressed as follows:

$$\{ZL_{channel}\langle...\rangle\}\cdot n(dye)_{adsorbed}$$
$$\rightleftharpoons \{ZL_{channel}\langle m\cdot dye\rangle\}\cdot(n-m)(dye)_{adsorbed} \quad (7)$$

Dyes that have not entered the channels are removed by washing the sample with a solvent that cannot displace the dyes located inside the channels. The type of solvent to use depends on the structure and the solubility of the dye. A property of the so-obtained dye−ZL composites that has to be considered is that they like to adsorb as much water as possible as soon as they are kept under ambient conditions. This can be accompanied by unwanted displacement of the dye from the channel to the outer surface of the ZL crystals, according to eq 8. Such a reaction is often accompanied by color change and luminescence quenching.[10,45] Plugging the channel entrances with stopcock molecules is used to avoid this leaking reaction.[10,22,43,46,47]

$$\{ZL_{channel}\langle n\cdot dye\rangle\} + xH_2O$$
$$\rightleftharpoons \{ZL_{channel}(m-y)dye, xH_2O\}\cdot y(dye)_{adsorbed} \quad (8)$$

Reaction 8 has been observed to be often reversible, that is, when water is removed, for example, by heating or evacuation, the dye goes back into to the channel.[45] Interestingly, neutral dyes bearing carbonyl groups are not so easily displaced by water. The reason for this was elucidated by performing extensive first-principles investigations on fluorenone inside ZL, both at dry conditions and in the presence of water. It was found that the interaction of the fluorenone carbonyl group with the zeolite extra framework potassium cations is responsible for the dye stabilization in ZL nanochannels. The result represents a general leitmotiv regarding important properties of carbonyl functionalized photoactive species in hydrophilic matrices.[40] This explains why the handling of HR, tb-DXP, and other dyes bearing accessible carbonyl groups is easier than in many other cases. Problems were, however, encountered when using strongly luminescent dyes that feature an ester group. It is difficult to handle the corresponding dye−ZL composites. The reason is that potassium−ZL channels containing some water become sufficiently acidic to cause hydrolysis of the esters.[32] Handling of guest molecules that can be protonated in the electronic ground or excited state can be also difficult for the same reason. It can lead to luminescence quenching or even destroy such dyes.[32] A moderate increase of the pH value inside the ZL channels can be achieved by the exchange of K^+ by Cs^+. The possibilities for reducing proton strength using metal cations are, however, limited. Furthermore, Cs^+ can enhance intersystem crossing, which is accompanied by fluorescence quenching.[39] Searching for alternatives, we found that exchanging some or all potassium cations by IMZ^+ yields excellent results, which we will now discuss. The comparison of the spectra, color, and fluorescence quantum yields measured under ambient conditions of different HR−ZL composites (Figure 3 and Table 2) illustrates the important influence of the substitution of metal cations by IMZ^+. This organic cation decreases the proton strength by decreasing the amount of metal cations that, according to eqs 3, 4, and 4a, are the origin of the Brönsted acidity in these systems. In addition to this, it is known that the imidazolium acts as a weak base.[22,48] The absorption spectrum of HR−NZL.5(Cs^+) is somewhat broadened with respect to that of HR−ZL.5(2.6K^+,1.0IMZ^+) and therefore appears to be a bit less red-shifted. The fluorescence maxima of both samples
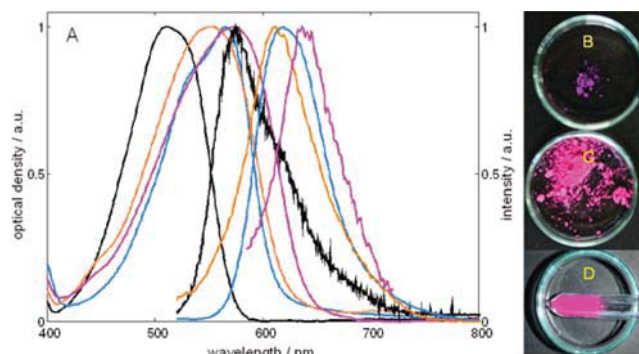

Figure 3. Spectra and colors of HR in different environments. (A) Absorption and fluorescence spectra; (black) 10^{-6} M solution in DCM, (pink) HR−ZL.5(K^+), (orange) HR−NZL.5(Cs^+), and (blue) HR−ZL.5(3.1K^+,0.5IMZ^+). All fluorescence spectra were excited at 490 nm. Spectra of the dye−ZL composites were measured as OGS. Photographic images taken under ambient conditions: (B) HR−ZL.5(3.6K^+) after exposure to ambient air, (C) HR−ZL.5(2.6 K^+,1.0IMZ^+) after exposure to ambient air, and (D) HR−ZL.5-(2.6K^+,1.0IMZ^+) that was left for 2 weeks in water. The color and luminescence of this sample did not change during this time.

Table 2. Luminescence Quantum Yield of Dye−ZL and Dye1,dye2−ZL Composites (Excitation Wavelength 490 nm) Measured as OGS

sample	co-cations	luminescence quantum yield (%)
HR−ZL.5	3.6 K^+	3
HR−NZL.5	3.6 Cs^+	21
HR−ZL.5	2.6 K^+, 1.0 IMZ^+	~100
tb-DXP,HR−ZL.01,.14	3.1 K^+, 0.5 IMZ^+	~100
tb-DXP,HR−ZL.01,.12	2.6 K^+, 1.0 IMZ^+	90
tb-DXP,HR−ZL.01,.09	3.6 IMZ^+	96

appear, however, at about the same wavelength, if we disregard the apparent slight red shift seen in the latter, which is caused by self-absorption. The major difference between these two samples is the fluorescence quantum yield (Table 2), which is 0.21 for HR−NZL.5(Cs^+) and approximately 1 for the IMZ^+ exchanged sample. The luminescence is heavily quenched in the HR−ZL.5 (3.6K^+) with a quantum yield of 0.03 only. The visual effect of this is illustrated in Figure 3B,C, which shows a comparison of photographic images taken at ambient conditions of HR−ZL.5(K^+) and HR−ZL.5(2.6 K^+,1.0 IMZ^+).

The low luminescence quantum yield of the all-metal cation based HR−ZL composites is the reason there was little interest in using HR as a chromophore for synthesizing antenna systems. The new possibility for tuning the proton activity inside the channels of ZL by substituting some or all of the metal cations by IMZ^+ has completely changed this situation. The fluorescence spectrum of tb-DXP−ZL overlaps very well with the absorption band of HR−ZL(3.5IMZ^+), as illustrated in Figure 4A. This results in a large spectral overlap integral and a Förster radius of nearly 8 nm.[49] This is due to the essentially parallel arrangement of the two transition moments and promises very efficient Förster resonance energy transfer (FRET). The type of antenna material we discuss here is sketched in Figure 1A. An important feature of dye−ZL composites is that sequential insertion of two different dyes 1 and 2 can be realized, leading to advanced supramolecular organization.[10,11,43,45]
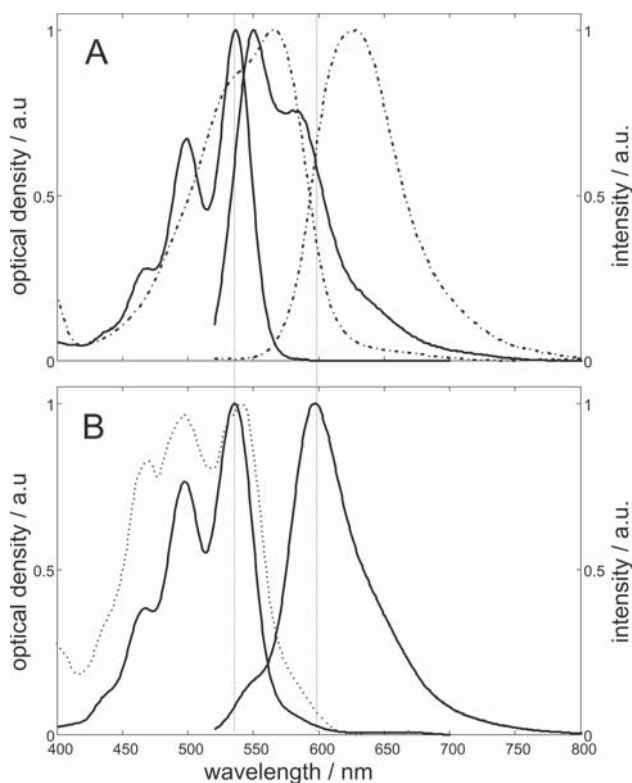
Figure 4. Absorption, fluorescence, and excitation spectra of dye−ZL composites measured as OGS. All fluorescence spectra were excited at 490 nm. The two vertical lines (solid, gray) help in comparing the spectra. (A) Spectra of tb-DXP−ZL.01(3.6K⁺) (solid) and of HR−ZL.5(3.1K⁺,0.5IMZ⁺) (dash−dot), measured as OGS. (B) Spectra of the antenna composite tb-DXP,HR−ZL.009,.25 (3.1K⁺,0.5IMZ⁺). The excitation spectrum (dotted line) was observed at 630 nm.

Sandwich-type composites featuring two dye types can be synthesized by sequential loading. One type of dye that absorbs light at shorter wavelengths is present in large excess and acts as donor (green) for acceptors (red) present in much lower amounts. We have chosen to first insert the acceptors (A) followed by the donors (D). This leads to D,A−ZL antenna composites, where D are at the entrances, and A in the middle part of the channels. Light is absorbed by the D and transported by means of FRET to the A. If efficient FRET from D to A is desired, the A's should be reached before the excited D's have time to decay by emitting light or any other radiationless decay channels. This limits the acceptable channel length and is why we have used barrel type crystals of about 500 nm length and diameter. In order to obtain chemically and photochemically stable materials, we found it necessary to plug the channel entrances with stopcock molecules as illustrated in Figure 1. This prevents the leakage of the guests and the entrance of the unwanted molecules that can lead to destruction of the composites when, for example, embedded in a polymer and exposed to higher temperature or light irradiation.

A typical result obtained by using tb-DXP as donors and HR as acceptors with a D/A ratio of 15.5:1 and 0.5 IMZ⁺ per unit cell, leading to a composite we name tb-DXP,HR−ZL.009,.25 (3.1K⁺,0.5IMZ⁺) is reported in Figure 4B. The extinction coefficients of tb-DXP and of HR are 88 200 M⁻¹cm⁻¹ (525 nm, DCM) and 20 000 M⁻¹cm⁻¹ (509 nm, DCM), respectively. This means that the ratio of the D/A absorption

maxima is about 120:1. The maximum of the HR absorption band in ZL is shifted to longer wavelength, as seen in Figure 3A. The ratio of the integrated acceptor to total fluorescence intensity was determined to be 0.87, which means that FRET efficiency is about 87%, a value that could be well reproduced by independently preparing several samples of the same composition. A consequence is that these tb-DXP,HR−ZL composites show very low self-absorption, which is highly important for using them in LSC devices,[1,11,50] as is the luminescence quantum yield which we report for three different tb-DXP,HR−ZLp$_A$,p$_D$((3.6 − x)K⁺,xIMZ⁺) in Table 2.

It is interesting that the fluorescence spectrum of HR shifts to shorter wavelength in all tb-DXP,HR−ZL composites with respect to the HR−ZL material. Furthermore, the vibrational substructure can be observed in the former, while it is absent in the latter. Comparison with the spectra given in Figure 3 indicates that its shape is similar to that observed in DCM. In order to understand this, it is important to realize that a loading of 0.009 means that on average two HR acceptor molecules are present in each channel, as illustrated in Figure 1. These are embedded in the middle of 66 donors (tb-DXP). This means that the HR feels, at least partially, embedded in the aliphatic organic environment offered by the tertiary butyl groups of tb-DXP, which favorably affects its properties. The excitation spectrum shown in Figure 4B indicates optical saturation, most probably present in the individual composite particles or in aggregates thereof. This effect and its consequences have been discussed by us recently in detail.[11]

The procedure described in the Experimental Section for plugging the channel entrances has no influence on the spectroscopic properties of the composites. The reaction conditions must, however, be chosen such that the solvent used to carry out the reaction does not wash out the guests. This is not a problem if tb-DXP is the molecule adjacent to the channel entrances. In Figure 5, we report results of a washing experiment for HR−ZL composites prepared with barrel type and nanosized ZL. The results show that HR can be washed out easily using a 1:1 mixture of acetonitrile/1-butanol, a solvent mixture that can be considered as representative. We see that
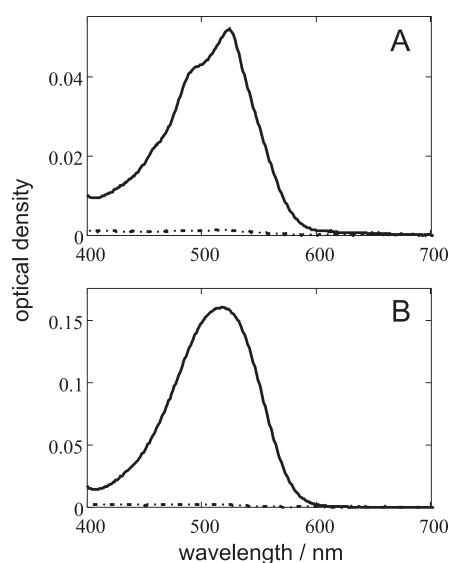
Figure 5. Absorption spectra of the washing solution of (solid line) open and (dash-dot) stopcock-plugged HR−ZL composites. (A) HR−ZL.5(3.6IMZ⁺), barrel type ZL. (B) nanosized HR−NZL.5(3.6Cs⁺).

rapid leakage of the unplugged samples is observed, while the plugged composites show no dye loss over the same time period. This also applies for tb-DXP−ZL and for tb-DXP,HR−ZL composites where no leakage was observed after storing the samples for several months. Similar results have been obtained when using (3-aminopropyl)triethoxysilane (APTES) for plugging the channel entrances.[10]

4. CONCLUSIONS

An important reason for instability, color change, and luminescence quenching of dyes inside the channels of ZL is often the high proton activity caused by exchangeable metal cations in the presence of water molecules (see eqs 4 and 4a, as well as the Supporting Information). The organic dye hostasol red (HR) is strongly luminescent in aprotic solvents but only weakly luminescent in potassium ZL at ambient conditions. We observed a dramatic increase of the luminescence quantum yield of HR−ZL composites if part or all of the exchangeable potassium cations per unit cell are substituted by IMZ$^+$ and if the acceptor HR is embedded in the middle part of the channels so that it is fully protected and feels the environment of the tb-DXP. Our observation led to the discovery of a highly efficient donor,acceptor-ZL antenna material with a perylene dye (tb-DXP) as donor and HR as acceptor, with a D/A absorption ratio of more than 100:1 and a FRET efficiency in the range of 90%.

In order to obtain materials with long-term chemical and photochemical stability, it is necessary to plug the channel entrances with stopper molecules. We described a successful procedure for achieving full sealing of the ZL channels. This new material is of great interest for applications in LSC devices because the efficiency killing self-absorption is very low and for any field in which robust, strongly luminescent particles are needed.

■ ASSOCIATED CONTENT

ⓢ Supporting Information

Detailed discussion of the effects of metal cations in the channels on the proton activity inside the ZL. This material is available free of charge

■ AUTHOR INFORMATION

Corresponding Authors
*E-mail: andre.devaux@unifr.ch.
*E-mail: peter.belser@unifr.ch.
*E-mail: gion.calzaferri@dcb.unibe.ch.

Author Contributions
The manuscript was written through contributions of all authors.

Notes
The authors declare no competing financial interest.

■ ACKNOWLEDGMENTS

■ REFERENCES

(1) Debije, M. G.; Verbunt, P. P. *Adv. Energy Mater.* **2012**, *2*, 12−35.
(2) Giovanella, U.; Leone, G.; Galeotti, F.; Mróz, W.; Meinardi, F.; Botta, Ch. *Chem. Mater.* **2014**, *26*, 4572−4578.
(3) Cucinotta, F.; Guenet, A.; Bizzarri, C.; Mróz, W.; Botta, Ch.; Milián-Medina, B.; Gierschner, J.; De Cola, L. *ChemPlusChem* **2014**, *79*, 45−57.
(4) Calzaferri, G.; Devaux, A. *Supramolecular Photochemistry: Controlling Photochemical Processes*; Ramamurthy, V., Inoue, Y., Eds.; John Wiley & Sons: Hoboken, NJ, 2011; Chapter 9, 285−387.
(5) Giansante, C.; Schäfer, C.; Raffy, R.; Del Guerzo, A. *J. Phys. Chem. C* **2012**, *116*, 21706−21716.
(6) Scholes, G. D.; Fleming, G. R.; Olaya-Castro, A.; van Grondell, R. *Nat. Chem.* **2011**, *3*, 763−774.
(7) Yong, C.; Parkinson, P.; Kondratuk, D. V.; Chen, W.; Stannard, A.; Summerfield, A.; Sprafke, J.; O'Sullivan, M.; Beton, P.; Anderson, H. L.; Herz, L.; *Chem. Sci.***2014**, DOI: 10.1039/C4SC02424A.
(8) Garo, F.; Häner, R. *Bioconjugate Chem.* **2012**, *23*, 2105−2113.
(9) Garg, V.; Kodis, G.; Liddell, P. A.; Terazono, Y.; Moore, T. A.; Moore, A. L.; Gust, D. *J. Phys. Chem. B* **2013**, *117*, 11299−11308.
(10) Calzaferri, G.; Huber, S.; Maas, H.; Minkowski, C. *Angew. Chem., Int. Ed.* **2003**, *42*, 3732−3758.
(11) Devaux, A.; Calzaferri, G.; Miletto, I.; Cao, P.; Belser, P.; Brühwiler, D.; Khorev, O.; Häner, R.; Kunzmann, A. *J. Phys. Chem. C* **2013**, *117*, 23034−23047.
(12) Hashimoto, S.; Moon, H. R.; Yoon, K. B. *Microporous Mesoporous Mater.* **2007**, *101*, 10−18.
(13) Prasetyanto, E. A.; Manini, P.; Napolitano, A.; Crescenzi, O.; d'Ischia, M.; De Cola, L. *Chem.—Eur. J.* **2014**, *20*, 1597−1601.
(14) Mahato, R. N.; Lülf, H.; Siekman, M. H.; Kersten, S. P.; Bobbert, P. A.; de Jong, M. P.; De Cola, L.; van der Wiel, W. G. *Science* **2013**, *341*, 257−260.
(15) Matsunaga, C.; Uchikoshi, T.; Suzuki, S.; Sakka, Y.; Matsuda, M. *Mater. Lett.* **2013**, *93*, 408−410.
(16) Wen, T.; Zhang, W.; Hu, X.; He, L.; Li, H. *ChemPlusChem.* **2013**, *78*, 438−442.
(17) Hüve, Z.; Li, J.; Krampe, C.; Luppi, G.; Tsotsalas, M.; Klingauf, J.; De Cola, L.; Riehemann, K. *Small* **2013**, *9*, 1809−1820.
(18) Szarpak-Jankowska, A.; Burgess, C.; De Cola, L.; Huskens, J. *Chem.—Eur. J.* **2013**, *19*, 14925−14930.
(19) Beierle, J. M.; Roswanda, R.; Erne, P. M.; Coleman, A. C.; Browne, W. R.; Feringa, B. L. *Part. Part. Syst. Charact.* **2013**, *30*, 273−279.
(20) Manzano, H.; Gartzia-Rivero, L.; Bañuelos, J.; López-Arbeloa, I. *J. Phys. Chem. C* **2013**, *117*, 13331−13336.
(21) Grüner, M.; Siozios, M. V.; Hagenhoff, B.; Breitenstein, D.; Strassert, C. A. *Photochem. Photobiol.* **2013**, *89*, 1406−1412.
(22) Li, P.; Wang, Y.; Li, H.; Calzaferri, G. *Angew. Chem., Int. Ed.* **2014**, *53*, 2904−2909.
(23) Baerlocher, Ch.; McCusker, L. B.; Olson, D. H.; *Atlas of Zeolite Framework Types*, 6th revised ed.; Elsevier: Amsterdam, 2007.
(24) Ohsuna, T.; Slater, B.; Gao, F.; Yu, J.; Sakamoto, Y.; Zhu, G.; Terasaki, O.; Vaughan, D. E.; Qiu, S.; Catlow, C. R. *Chem.—Eur. J.* **2004**, *10*, 5031−5040.
(25) Farneth, W. E.; Gorte, R. J. *Chem. Rev.* **1995**, *95*, 615−635.
(26) Eichler, U.; Brändle, M.; Sauer, J. *J. Phys. Chem. B* **1997**, *101*, 10035−10050.
(27) Ryder, J. A.; Chakraborty, A. K.; Bell, A. T. *Phys. Chem. B* **2000**, *104*, 6998−7011.
(28) Zecchina, A.; Spoto, G.; Bordiga, S. *Phys. Chem. Chem. Phys.* **2005**, *7*, 1627−1642.
(29) Meeprasert, J.; Jungsuttiwong, S.; Namuangruk, S. *Microporous Mesoporous Mater.* **2013**, *175*, 99−106.
(30) Calzaferri, G.; Gfeller, N. *J. Phys. Chem.* **1992**, *96*, 3428−3435.
(31) Corrent, S.; Hahn, P.; Pohlers, G.; Connolly, T. J.; Scaiano, J. C.; Fornés, V.; García, H. *J. Phys. Chem. B* **1998**, *102*, 5852−5858.
(32) Albuquerque, R. Q.; Calzaferri, G. *Chem.—Eur. J.* **2007**, *13*, 8939−8952.
(33) Bussemer, B.; Dreiling, I.; Grummt, U. W.; Mohr, G. J. *J. Photochem. Photobiol., A* **2009**, *204*, 90−96.
(34) Rademacher, A.; Märkle, S.; Langhals, H. *Chem. Ber.* **1982**, *115*, 2927−2934.

(35) Zabala Ruiz, A.; Brühwiler, D.; Ban, T.; Calzaferri, G. *Monatsh. Chem.* **2005**, *136*, 77−89.

(36) Larlus, O.; Valtchev, V. P. *Chem. Mater.* **2004**, *16*, 3381−3389.

(37) Calzaferri, G.; Méallet-Renault, R.; Brühwiler, D.; Pansu, R.; Dolamic, I.; Dienel, T.; Adler, P.; Li, H.; Kunzmann, A. *ChemPhysChem* **2011**, *12*, 580−594.

(38) Fois, E.; Tabacchi, G.; Devaux, A.; Belser, P.; Brühwiler, D.; Calzaferri, G. *Langmuir* **2013**, *29*, 9188−9198.

(39) Ramamurthy, V. Photoprocesses of Organic Molecules Included in Zeolites. In *Photochemistry in Organized and Constrained Media*; Ramamurthy, V., Ed.; VCH Publishers: New York, 1991, 429−493.

(40) Fois, E.; Tabacchi, G.; Calzaferri, G. *J. Phys. Chem. C* **2010**, *114*, 10572−10579.

(41) Hawkes, S. T. *J. Chem. Educ.* **1996**, *73*, 516−517.

(42) Barrer, R. M *Zeolites and Clay Minerals as Sorbents and Molecular Sieves*; Academic Press: London, 1978.

(43) Calzaferri, G. *Langmuir* **2012**, *28*, 6216−6231.

(44) Fois, E.; Tabacchi, G.; Calzaferri, G. *J. Phys. Chem. C* **2012**, *116*, 16748−16799.

(45) Pauchard, M.; Devaux, A.; Calzaferri, G. *Chem.—Eur. J.* **2000**, *6*, 3456−3470.

(46) Brühwiler, D.; Calzaferri, G.; Torres, T.; Ramm, J. H.; Gartmann, N.; Dieu, L.-Q.; López-Duarte, I.; Martínez-Díaz, M. V. *J. Mater. Chem.* **2009**, *19*, 8040−8067.

(47) López-Duarte, I.; Dieu, L.-Q.; Dolamic, I.; Martínez-Díaz, M. V.; Torres, T.; Calzaferri, G.; Brühwiler, D. *Chem.—Eur. J.* **2011**, *17*, 1855−1862.

(48) Klähn, M.; Seduraman, A.; Wu, P. *J. Phys. Chem. B* **2011**, *115*, 8231−8241.

(49) Förster, T. *Naturwissenschaften* **1946**, *6*, 166−175.

(50) Dienel, T.; Bauer, C.; Dolamic, I.; Brühwiler, D. *Sol. Energy* **2010**, *84*, 1366−1369.

■ NOTE ADDED AFTER ASAP PUBLICATION

This paper was published ASAP on November 26, 2014, with an error to equation 4a and equation 5. The corrected version reposted with the issue on December 9, 2014.